

CHAPTER 35

NON-REFLECTED MULTI DIRECTIONAL WAVE MAKER THEORY AND EXPERIMENTS OF VERIFICATION

Kazunori ITO¹ , Hidehiro KATSUI², Masashi MOCHIZUKI³, Masahiko ISOBE⁴

ABSTRACT

In the hydraulic model test in a wave basin, reflected waves from models of structures and walls of the basin reflect again at the wave maker. The re-reflected waves disturb wave field in the basin and consequently reduce the accuracy of experiments. We developed a non-reflected multi directional wave maker theory. By taking into account both current and past water elevation data in front of the wave paddles, the theory makes the wave makers possible to absorb reflected multi directional waves. Numerical simulations and experiments show that this theory is superior to the conventional theory in its efficiency of the absorption.

1. INTRODUCTION

In general, multi directional wave experiments using wave makers placed in a line have the following problems: an experiment area with a uniform wave field is small, and reflected waves from a model and/or a wave basin cannot be absorbed efficiently. In order to create a larger experiment area, reflecting walls are installed at the end of multi directional wave makers placed in a line[1], or wave makers are set in the J-shape[2]. These methods are very effective to enlarge an experiment area. However, when a model is surrounded by wave makers and/or a reflecting wall, re-reflected waves from these wave makers and/or a reflecting wall exert a large effect on the model; thus, it becomes important to absorb reflected waves. The method proposed by Kawaguchi[3], which uses the data on water surface elevation at the wave paddle front, has been put to a practical use for absorbing uni- directional reflected waves. Hiraguchi et al.[4] carried out experiments by applying this method to multi-directional wave makers to absorb multi-directional waves. However, as only an orthogonal wave direction against a wave paddle is taken into account in Kawaguchi's method, the absorptivity decreases when the incidence angle of reflected waves is oblique. Ikeya et al.[5] proposed the method

¹ M.Eng, Taisei Corporation, Wakasu-Nai, Koto-Ku, Tokyo, Japan 136

² Dr.Eng, Manager, Hydraulic Section, Technology Research Center, Taisei Corporation
Nase-machi 344-1, Totsuka-Ku, Yokohama-City, Kanagawa, Japan 245

³ Deputy Section Chief, Akishima Eng. Dept., Advanced Machines And Systems, Div., Mitsui
Engineering and Ship Building Co., LTD
Tsutsujigaoka1-1-50, Akishima-City Tokyo, Japan 196

⁴ Professor, Dr.Eng, Dept. of Civil Engineering, University of Tokyo
Hongo-7-3-1, Bunkyo-Ku, Tokyo, Japan 113

for absorbing oblique waves using the data on water surface elevation at the front of two or more wave paddles. However, the absorptivity in this method also decreased due to the errors in computing reflected waves, as evanescent waves are not taken into account. Their theory does not have a wide application, because it stands on the assumption that a wave basin has side walls. Besides, as the above two methods take only a representative frequency into account, the absorptivity decreases when a wave has dominant frequency dispersion.

This paper aims to establish a non-reflected wave maker theory for multi-directional waves in consideration of directional dispersion, frequency dispersion and evanescent waves[6], and to report the results of the basic experiments on oblique regular waves to verify the theory[7].

2. FORMULATION OF NON-REFLECTED WAVE MAKER THEORY

Fig. 1 shows the coordinates used in the analysis: x- and y-axes in the horizontal direction, and z-axis in the vertical upward direction.

Wave paddles are set along the x-axis. Here, let us take a piston-type wave maker by way of example to develop the theory.

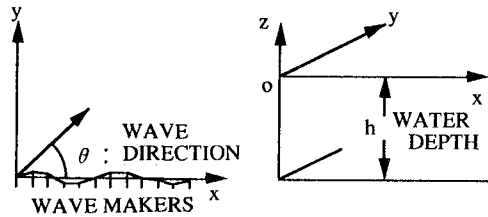


Fig.1 Definition of coordinate

2.1. WAVE MAKER THEORY

The fluid treated here is inviscid and unconsolidated. When a small amplitude wave theory can be applied to the wave and the amplitude of a wave paddle is small enough, the problems of wave making with the constant water depth are governed by the following equations:

$$\frac{\partial^2 \Phi}{\partial x^2} + \frac{\partial^2 \Phi}{\partial y^2} + \frac{\partial^2 \Phi}{\partial z^2} = 0 \tag{1}$$

$$\frac{\partial \Phi}{\partial t} + g\eta = 0 \tag{2}$$

: z = 0

$$\frac{\partial \eta}{\partial t} - \frac{\partial \Phi}{\partial z} = 0 \tag{3}$$

: z = 0

$$\frac{\partial \Phi}{\partial n} = \frac{\partial X}{\partial t} \tag{4}$$

: y = 0

$$\frac{\partial \Phi}{\partial z} = 0 \tag{5}$$

: z = -h

where, $\Phi(x,y,z,t)$: velocity potential, $\eta(x,y,t)$: water surface elevation, g : gravity acceleration, h : water depth, n : normal direction, X : displacement of a wave paddle.

Now, the theory is developed for regular waves. By separating a variable Φ , Eq.(6) can be obtained from Eq.(1) and (5).

$$\Phi(x,y,z,t) = \sum_{n=0}^{\infty} \phi_n(x,y) \frac{\cosh[k_n(z+h)]}{\cosh k_n h} e^{-i\omega t} \tag{6}$$

When $n=0$, angular frequency ω and a wave number kn in Eq.(6) satisfy the

dispersion relation Eq.(7) of a progressive wave component; when $n=1$ to ∞ , they satisfy the dispersion relation Eq.(8) of an evanescent wave component. Here, k_n is an imaginary number when $n=1$ to ∞ , and \hat{k}_n is the imaginary part of k_n .

$$\omega^2 = gk_n \tanh k_n h \tag{7}$$

$$\omega^2 = -g\hat{k}_n \tan \hat{k}_n h \tag{8}$$

Next, use Eq.(4) as follows:

$$\left. \frac{\partial \Phi}{\partial n} \right|_{y=0} = \frac{\partial \Phi}{\partial y} = U(x,y)F(z)e^{-i\omega t} \tag{9}$$

where, $U(x,y)$: amplitude of wave paddle velocity $F(z)$: function of wave paddle motion ($F(z)$ of a piston-type wave maker = 1)

By substituting Eq.(6) into Eq.(9) and integrating in the vertical direction using orthogonality, Eq.(10) can be obtained as follows:

$$U = \frac{D_n}{G_n} \frac{\partial \phi_n}{\partial y} \tag{10}$$

In the case of a piston-type wave maker, D_n and G_n can be obtained as follows, respectively.

$$D_n = \frac{\tanh k_n h}{2k_n} \left[1 + \frac{2k_n h}{\sinh 2k_n h} \right] : n = 0 \quad , \quad = \frac{\tan \hat{k}_n h}{2\hat{k}_n} \left[1 + \frac{2\hat{k}_n h}{\sin 2\hat{k}_n h} \right] : n = 1, 2, 3, \dots \tag{11}$$

$$G_n = \frac{\tanh k_n h}{k_n} : n = 0 \quad = \frac{\tan \hat{k}_n h}{\hat{k}_n} : n = 1, 2, 3, \dots \tag{12}$$

If water surface elevation η_p of a progressive wave component is given as Eq.(13), U which is necessary for making a progressive wave can be determined as Eq.(14) from Eq.(10) with $y=0$.

$$\eta_p = a e^{i\{k_0(x \cos \theta + y \sin \theta) - \omega t\}} \tag{13}$$

$$U(x,0) = \frac{D_0}{G_0} \frac{g a k_0}{\omega} \sin \theta e^{i\{k_0(x \cos \theta)\}} \tag{14}$$

where, the subscript 0 represents a progressive wave, and a represents a complex amplitude of component waves.

ϕ_n of an evanescent wave is the solution of Eq.(15) and the boundary condition $\lim_{y \rightarrow \infty} \phi_n = 0$; then, from the relation in Eq.(10), Eq.(16) can be obtained.

$$\frac{\partial^2 \phi_n}{\partial x^2} + \frac{\partial^2 \phi_n}{\partial y^2} - \hat{k}_n^2 \phi_n = 0 \tag{15}$$

$$\phi_n = -\frac{D_0 G_n}{D_n G_0} \frac{g a k_0 \sin \theta}{\omega \sqrt{\hat{k}_n^2 + k_0^2 \cos^2 \theta}} e^{i k_0 x \cos \theta - y \sqrt{\hat{k}_n^2 + k_0^2 \cos^2 \theta}} \tag{16}$$

Therefore, when making a regular wave, the water surface elevation η_e of an

evanescent wave component at the wave paddle front ($y=0$) can be described as follows:

$$\eta_e(x, 0, t) = -\frac{D_0 G_n}{D_n G_0} \frac{ik_0 \sin \theta}{\sqrt{\hat{k}_n^2 + k_0^2 \cos^2 \theta}} e^{ik_0 x \cos \theta - i\omega t} \quad (17)$$

Thus, the water surface elevation at the wave paddle front can be obtained by adding the water surface elevation of a progressive wave component and that of an evanescent wave component as in Eq.(18):

$$\eta(x, 0, t) = \left[1 - \frac{D_0 G_n}{D_n G_0} \frac{ik_0 \sin \theta}{\sqrt{\hat{k}_n^2 + k_0^2 \cos^2 \theta}} \right] a e^{ik_0 x \cos \theta - i\omega t} \quad (18)$$

Multi-directional waves can be described as superposition of component waves. Therefore, the wave paddle velocity $A^{(i)}(x, y = 0, t)$ and the water surface elevation at the wave paddle front $\eta^{(i)}$ are obtained in Eq.(19) and (20), respectively.

$$\left. \frac{\partial \Phi}{\partial n} \right|_{y=0} = A^{(i)} = \sum_{j=1}^{\infty} \frac{D_{j0}}{G_{j0}} \frac{g a_j k_{j0}}{\omega_j} \sin \theta_j e^{i\{k_{j0}(x \cos \theta_j) - \omega_j t\}} \quad (19)$$

$$\eta^{(i)}(x, 0, t) = \sum_{j=1}^{\infty} \left[1 - \sum_{n=1}^{\infty} \frac{G_{jn} D_{j0}}{G_{j0} D_{jn}} \frac{ik_{j0} \sin \theta_j}{\sqrt{\hat{k}_{jn}^2 + k_{j0}^2 \cos^2 \theta_j}} \right] \times a_j e^{i(k_{j0} x \cos \theta_j - \omega_j t)} \quad (20)$$

Both the actual wave paddle velocity and water surface elevation are real variables, thereby becoming the real parts in Eq.(19) and (20). Hereafter, a symbol $\tilde{\sim}$ in this paper stands for a real variable.

2.2. ABSORPTION THEORY

The conventional non-reflected wave maker theory[3],[5], where the water surface elevation measured at the wave paddle front is converted into a wave making signal, is based on a so-called feedback control. This method has a great advantage in the aspect of practical control. This paper develops a new non-reflected wave maker theory using the data on water surface elevation at the wave paddle front.

In the case of non-reflected wave making, the water surface elevation at the wave paddle front ($\tilde{\eta}^{(m)}$) is the sum of the water surface elevation of a progressive wave which is a target wave ($\tilde{\eta}_p^{(i)}$), the water surface elevation of an evanescent wave which is created due to wave making ($\tilde{\eta}_e^{(i)}$), the water surface elevation of a progressive wave component of a reflected wave ($\tilde{\eta}_p^{(r)}$), and the water surface elevation of an evanescent wave which is created due to the motion of wave paddle to absorb a reflected wave ($\tilde{\eta}_e^{(r)}$); that is, ($\tilde{\eta}^{(m)} = \tilde{\eta}_p^{(i)} + \tilde{\eta}_e^{(i)} + \tilde{\eta}_p^{(r)} + \tilde{\eta}_e^{(r)}$). As $\tilde{\eta}^{(i)}$ ($= \tilde{\eta}_p^{(i)} + \tilde{\eta}_e^{(i)}$) can be calculated by Eq.(20), a reflected wave $\tilde{\eta}^{(r)}$ ($= \tilde{\eta}_p^{(r)} + \tilde{\eta}_e^{(r)}$) can be obtained as $\tilde{\eta}^{(r)} = \tilde{\eta}^{(m)} - (\tilde{\eta}_p^{(i)} + \tilde{\eta}_e^{(i)})$, where no re-reflection occurs from the wave paddle since reflected waves are absorbed.

The relation between the water surface elevation $\tilde{\eta}^{(r)}$ at the wave paddle

front which includes an evanescent wave and the wave paddle velocity $\tilde{A}^{(r)}$ is defined by transfer function $H_{pe}(\omega, \theta)$ as $\tilde{A}^{(r)}(x, 0, t) = H_{pe}(\omega, \theta) \tilde{\eta}^{(r)}(x, 0, t)$ in the case of a regular wave. The concrete form of $H_{pe}(\omega, \theta)$ is described in the following equation, which uses the real parts in Eq.(19).

$$H_{pe}(\omega, \theta) = \frac{D_0}{G_0} \frac{gk_0}{\omega} \sin \theta \times \left\{ 1 + \left(\sum_{n=1}^{\infty} \frac{D_n G_n}{D_n G_0} \frac{k_0 \sin \theta}{\sqrt{\hat{k}_n^2 + k_0^2 \cos^2 \theta}} \right)^2 \right\}^{-\frac{1}{2}} \quad (21)$$

Assuming that a reflected wave $\tilde{\eta}^{(r)}$ is in a narrow band spectrum of frequency and wave direction, Eq.(22) and (23) can be obtained as follows:

$$\tilde{\eta}^{(r)}(x, y, t) = \sum_{m=1}^{\infty} \tilde{a}_m \cos \varphi_m \quad (22)$$

$$\varphi_m = (\bar{k} + \Delta k_m) \left[x \cos(\bar{\theta} + \Delta \theta_m) - y \sin(\bar{\theta} + \Delta \theta_m) \right] - (\bar{\omega} + \Delta \omega_m) t + \varepsilon_m \quad (23)$$

where, ε_m is a phase number.

When $H_{pe}(\omega, \theta)$ can be expanded around a representative frequency $\bar{\omega}$ and a representative wave direction $\bar{\theta}$ using Taylor expansion in consideration of the first order quantity, the motion velocity of a wave paddle which absorbs reflected waves can be obtained in Eq.(24).

$$\tilde{A}^{(r)}(x, 0, t) = \bar{H}_{pe} \sum_{m=1}^{\infty} \tilde{a}_m \cos \varphi_m + \frac{\partial \bar{H}_{pe}}{\partial \omega} \times \sum_{m=1}^{\infty} \Delta \omega_m \tilde{a}_m \cos \varphi_m + \frac{\partial \bar{H}_{pe}}{\partial \theta} \sum_{m=1}^{\infty} \Delta \theta_m \tilde{a}_m \cos \varphi_m \quad (24)$$

Then, by obtaining a series of the second and third terms in the right side of Eq.(24) using simultaneous equations of $\tilde{\eta}^{(r)}$, $\partial^2 \tilde{\eta}^{(r)} / \partial t^2$ and $\partial^2 \tilde{\eta}^{(r)} / \partial x \partial t$ in consideration of the first order quantity, the motion velocity of a wave paddle can be expressed as follows:

$$\begin{aligned} \tilde{A}^{(r)} = & \bar{H}_{pe} \tilde{\eta}^{(r)} + \frac{\partial H_{pe}}{\partial \omega} \left\{ \frac{1}{2\bar{\omega}} \left(-\bar{\omega}^2 \tilde{\eta}^{(r)} - \frac{\partial^2 \tilde{\eta}^{(r)}}{\partial t^2} \right) \right\} \\ & + \frac{\partial H_{pe}}{\partial \theta} \left\{ \frac{1}{2} \left(1 - \frac{\bar{c}}{\bar{c}_g} \right) \cot \bar{\theta} \tilde{\eta}^{(r)} - \frac{1}{2\bar{\omega}^2} \left(1 + \frac{\bar{c}}{\bar{c}_g} \right) \right. \\ & \left. \times \cot \bar{\theta} \frac{\partial^2 \tilde{\eta}^{(r)}}{\partial t^2} - \frac{1}{\bar{k} \bar{\omega} \sin \bar{\theta}} \frac{\partial^2 \tilde{\eta}^{(r)}}{\partial x \partial t} \right\} \end{aligned} \quad (25)$$

where, \bar{k} : wave number of a progressive wave against $\bar{\omega}$
 \bar{c} : phase velocity of a progressive wave against $\bar{\omega}$
 \bar{c}_g : group velocity of a progressive wave against $\bar{\omega}$
 \bar{H}_{pe} : transfer function regarding a representative value

The second term in the right side of Eq.(25) is a correction term for frequency dispersion, and the third term is a correction term for directional dispersion.

From the above equations, the wave paddle velocity $\tilde{A}^{(r)}$ for absorbing can be calculated from a reflected wave; then, by subtracting $\tilde{A}^{(r)}$ from the wave paddle velocity $\tilde{A}^{(i)}$ for making a target wave, a wave paddle can be controlled. Thus, non-reflected wave making becomes possible.

3. DISCUSSION ON THE THEORY THROUGH NUMERICAL CALCULATION

3.1. DISCUSSION ON AN EVANESCENT WAVE

An evanescent wave occurs due to the difference between the wave paddle motion and a vertical distribution of horizontal water particle velocity of the target wave. The amplitude of an evanescent wave becomes largest at the wave paddle front, and decreases in accordance with the distance from a wave paddle.

Fig. 2 shows the ratio of progressive wave amplitude and evanescent wave amplitude, when a regular wave is created using a piston-type wave maker. From the figure, it is clear that when a piston-type wave maker creates a deep-sea wave with the large ratio of wavelength and water depth kh , an evanescent wave is more likely to occur; while, as the wave direction is tilted, it occurs less frequently.

Therefore, in the control method where a reflected wave is detected by using the water surface elevation at the wave paddle front, an evanescent wave must not be neglected. By taking into account of this wave, the absorption of a reflected wave is expected to be improved.

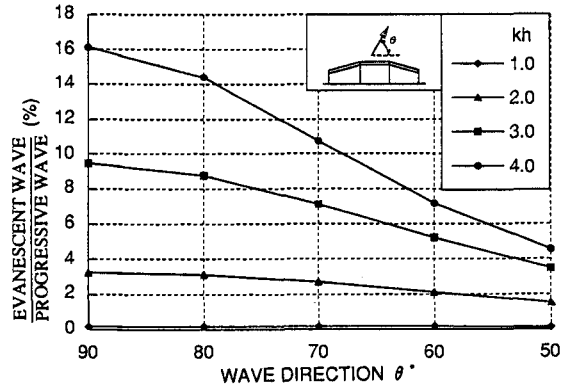


Fig.2 The ratio of progressive wave amplitude and evanescent wave amplitude

3.2. DISCUSSION ON NON-REFLECTED CONTROL

In a practical use of a reflected wave absorption control, a reflected wave is detected by a wave gauge installed on the wave paddle front as in conventional methods. Therefore, the differential of the theoretical equation(25) is necessarily approximated with finite- differential. Besides, it is not easy to give a representative wave direction in advance. For some structural models, a representative wave direction of a reflected wave is particularly difficult to predict. In the case of a floating model, wave direction of a reflected wave reaching a wave paddle varies from hour to hour according to the motion of the model. Here, a practical calculation method is adopted; as for a representative frequency, a representative value of the wave to be created is given in advance, and a representative wave direction is approximated using Eq.(26) and (27).

$$\theta(t) = \cos^{-1} \left[-\bar{c} \frac{\partial \tilde{\eta}^{(r)} / \partial x}{\partial \tilde{\eta}^{(r)} / \partial t} \right] \tag{26}$$

$$\bar{\theta}(t) = \frac{1}{N} \left[(N-1) \bar{\theta}(t - \Delta t) + \theta(t) \right] \tag{27}$$

where, $\theta(t)$: wave direction at the time t
 $\bar{\theta}(t)$: a representative wave direction

N is the value obtained by dividing the elapsed time of absorption control of reflected waves by the intervals of sampling of water surface elevation (Δt), that is, the number of times of sampling. $\partial/\partial x$ is the mean finite-differential of the second order, which is calculated from the data on water surface elevation at the front of two or more wave paddles. When $\partial/\partial t$ is defined as the unilateral finite-differential of the second order and $\partial^2/\partial t^2$ is as the unilateral finite-differential of the first order, they can be calculated from the data on water surface elevation measured in the past using a water gauge. As shown above, the characteristic of absorption control in this theory is the use

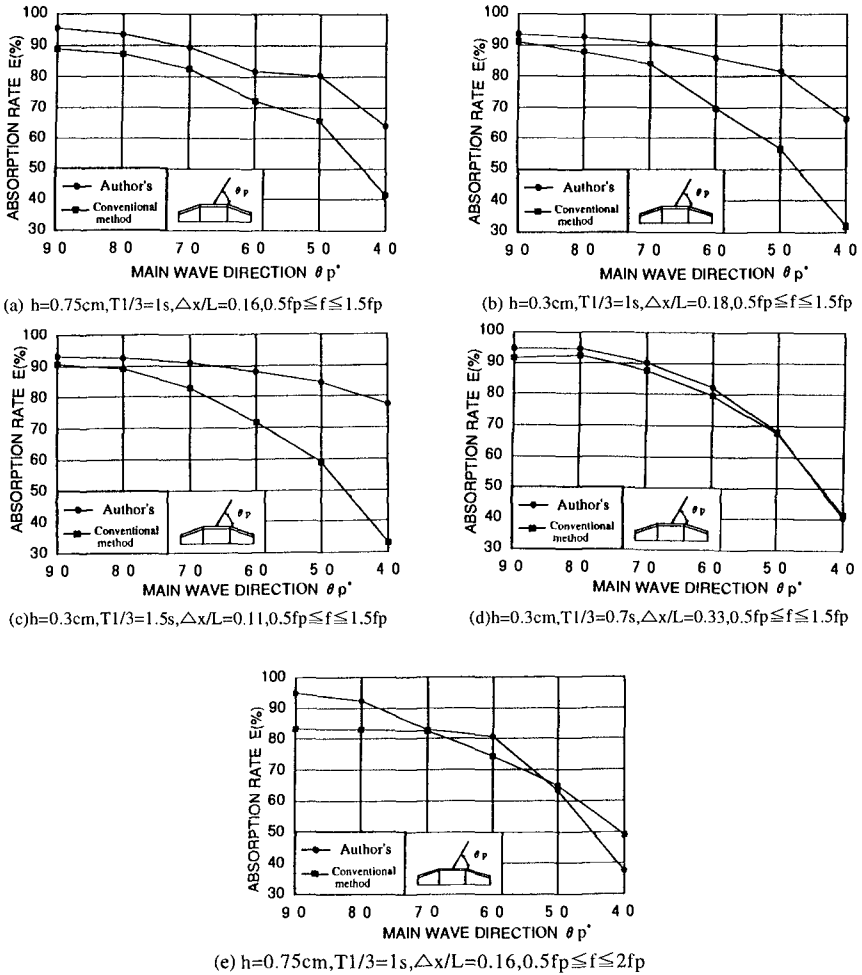


Fig.3 The comparison of the absorption rate between Author's method and Conventional method

of data on water surface elevation at the wave paddle front and the past data. As a result of numerical calculation without approximating the derivation in Eq.(25), this theory was proved valid regardless of a wave direction or water depth. Next, by approximating the derivation in Eq.(25), numerical calculation was conducted. The conditions of a reflected wave include Bretschneider-Mitsuyasu spectrum, Mitsuyasu-type directional function ($S_{max}=10$), significant wave height 3cm, significant wave period 0.7s, 1.0s, 1.5s, and the water depth 0.3m, 0.75m. Wave direction against the peak wave direction is in the range of $\pm 30^\circ$. The frequency range is 0.5 to 1.5 times and 0.5 to 2.0 times as large as the peak frequency f_p . The intervals of wave gauges (Δx) is 0.25m, and Δt is given as 0.01s. Using these, it is quantitatively examined using the absorption rate E which is defined by Eq.(28).

$$E = \left[1 - \frac{\sqrt{\left(\int_0^T (\tilde{A}_r(x,0,t) - \tilde{A}_n(x,0,t))^2 dt \right)}}{\left(\int_0^T \tilde{A}_r(x,0,t)^2 dt \right)} \right] \times 100 \% \tag{28}$$

where, $\tilde{A}_r(x,0,t)$: the wave paddle velocity in Eq.(19)

$\tilde{A}_n(x,0,t)$: the wave paddle velocity in Eq.(25)

For comparison, the results of conventional method are also shown: in the conventional method, there are no second and third terms in the right side of Eq.(25); $\sin \theta$ in the right side of transfer function equation(21) is 1; and the total series is 0.

Fig.3 shows the comparison of the absorption rate when the peak frequency of a reflected wave, water depth and the frequency range are varied. From (a) and (b), it is clear that when the peak frequency is 1s, this theory is superior to the conventional method in terms of absorptivity, regardless of the water depth. When frequency becomes 1.5s as in (c), the ratio of the wave gauge space and the wavelength ($\Delta x/L$) becomes smaller and the approximation becomes more accurate, thereby improving the absorptivity. On the other hand, in (d) where frequency is 0.7s and the water depth is 0.3m, the accuracy of approximation decreases, showing no significant difference from the conventional method. Therefore, when the frequency range of reflected waves is about 0.5 to 1.5 times as large as f_p , this theory is significant on condition that $\Delta x/L$ is 0.33 or smaller. In (e) where the frequency range is larger (0.5 to 2.0 times as large as f_p), this theory exceeds the conventional method on condition that the wave direction is around 90° ; however, as the wave direction is tilted, there becomes no difference from the conventional method. This is caused by the limit in assuming a narrow band spectrum and the error in approximation.

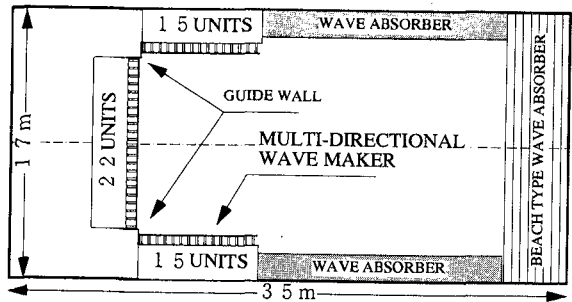


Fig.4 The C-shape multi directional wave makers

4. EXPERIMENTS ON REFLECTED WAVE ABSORPTION

4.1. EXPERIMENTAL EQUIPMENT AND METHOD

(1) EXPERIMENTAL EQUIPMENT

A multi-directional wave maker is a multiplex piston-type wave maker, consisting of 52 wave makers. Two capacitance-type wave gauges were installed with a space of 25cm on a 50cm-wide wave paddle: one at the front of a driving shaft, the other in the middle of two driving shafts. As shown in Fig.4, multi-directional wave makers were arranged in the C-shape within a wave basin (35×24m). The number of wave makers on each side was 15, 22, and 15, respectively. The L-shape installation is also possible: 30 wave makers on the long side and 22 on the short side of the wave basin. Cut-off walls called guide walls were installed at each corner of the C-shape. The neutral point of each wave paddle can be shifted arbitrarily within the range of $\pm 40\text{cm}$ stroke. The power of each driving shaft can also be adjusted arbitrarily.

(2) EXPERIMENTAL METHOD

The experiment was carried out by making waves from WAVE MAKER 1 and 2 shown in Fig.5, with the WAVE MAKER 3 serving as absorption control as in Eq.(25). Following the method proposed by Toida et al.[8], the power of five driving shafts installed at the ends of the wave makers 1 and 2 (C, F) was controlled to be 100% to 0%, in order to decrease the effect of diffraction waves from the ends. In addition, in order to decrease the effect of diffraction waves from the corner, the method of shifting the neutral point of wave paddles[7] was adopted. In absorption control in Eq.(25), both ends were controlled for the purpose of decreasing diffraction waves.

The water surface elevation at the front of WAVE MAKER 3 was measured at the lattice points (24×15) with a 30cm-space, as described by hatching in Fig.5.

4.2. DISCUSSION ON AN EVANESCENT WAVE

Regular waves were made in the vertical direction from the wave makers 2 in Fig.5, then both the water surface elevation at the wave paddle front and an evanescent wave were measured. The measurement conditions were: frequency changing from 0.7s to 1.0s and 1.5s, water depth from 50cm to 60cm, 70cm and 80cm, and wave height from 0.5cm to 0.8cm.

Fig.6 shows the relation of the ratio of wavelength and water depth kh and the amplitude

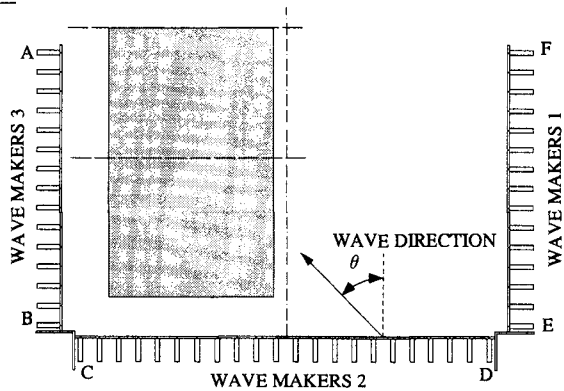


Fig.5 Measurement area and definition of wave direction

Fig.6 shows the relation of the ratio of wavelength and water depth kh and the amplitude

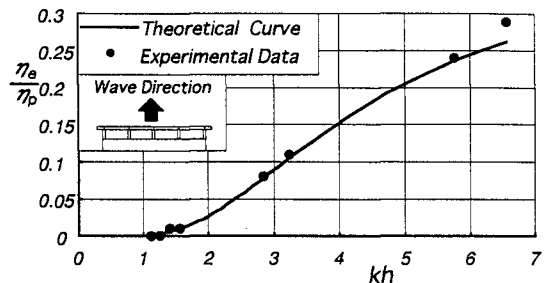
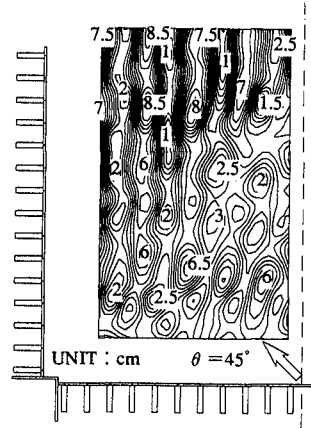


Fig.6 The comparison between theoretical evanescent wave and experimental one

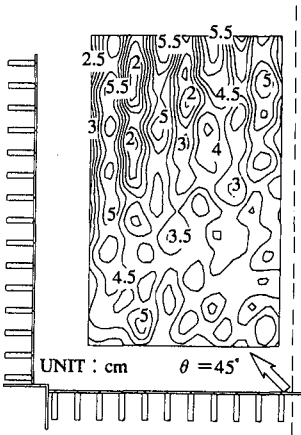
ratio of a progressive wave component and an evanescent wave component η / η_p when $\theta = 0^\circ$, along with the theoretical curve for comparison. It is clear from the figure that the experimental values agree well with the theoretical values. When $kh < 2$, η / η_p was less than 0.02 which can be disregarded; whereas when $kh > 3$, it can no more be disregarded. Since an evanescent wave is also a wave direction function, the more the wave direction became oblique, the smaller the value of η / η_p became. For example, when water depth was 80cm, frequency 1.0s, and wave direction 45° , η / η_p was about 0.03.

4.3. CAPABILITY OF NON-REFLECTED WAVE MAKER THEORY FOR REGULAR WAVES

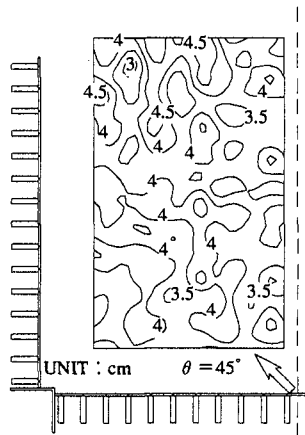
Fig.7 shows the wave height distribution when absorption control on the WAVE MAKER 3 was conducted against an incident wave with frequency 1.0s, wave direction 45° , wave height 5cm, and water depth 80cm. For comparison, Fig.7 also shows the case where the WAVE MAKER 3 was fixed to serve as a reflecting wall and the results of conventional method. When the WAVE MAKER 3 absorbed an incident wave, created waves formed a wave field; when it did not, incident waves and reflected waves formed a two-directional standing wave field. In Fig.7(a), a standing wave field was formed at the front of the WAVE MAKER 3; in (b) where wave direction was disregarded, though the wave height fluctuation became smaller, a standing wave field was also formed. This means that absorptivity decreased because the wave direction was disregarded. On the other hand, in (c) where



(a) Reflecting wall



(b) Conventional method



(c) Author's method

Fig.7 The contour of the wave heights
(Regular wave: T=1s, H=5cm, $\theta = 45^\circ$)

absorption control was conducted using Eq.(25), the wave height distribution showed uniformity. However, around A, at the end of the wave makers, showed a tendency to form a standing wave field.

Fig.8 shows the similar results, when frequency was given as 1.5s. The absorptivity by Eq.(25) was high.

(Regular wave: $T=1s, H=5cm, \theta=45^\circ$) Fig.9 shows the results when the wave direction was 60° . Though the pattern of isolines was slightly different, there was no significant difference in the region where a standing wave field was formed and in the isoline

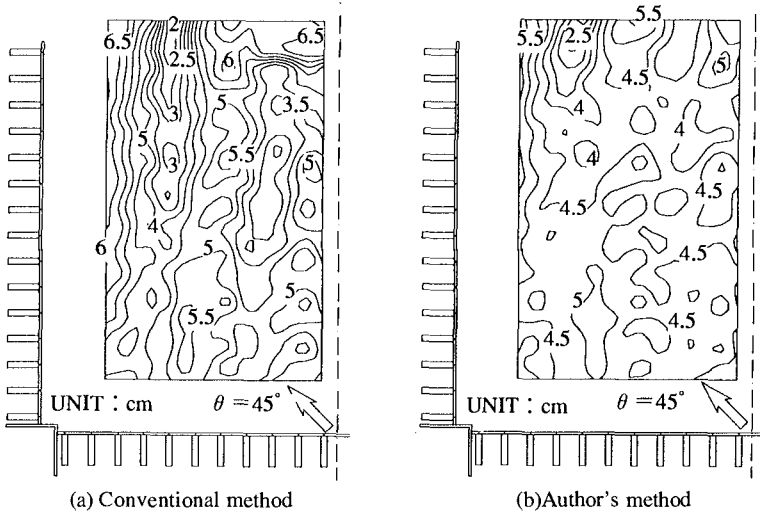


Fig.8 The contour of the wave heights
Regular wave: $T=1.5s, H=5cm, \theta=45^\circ$)

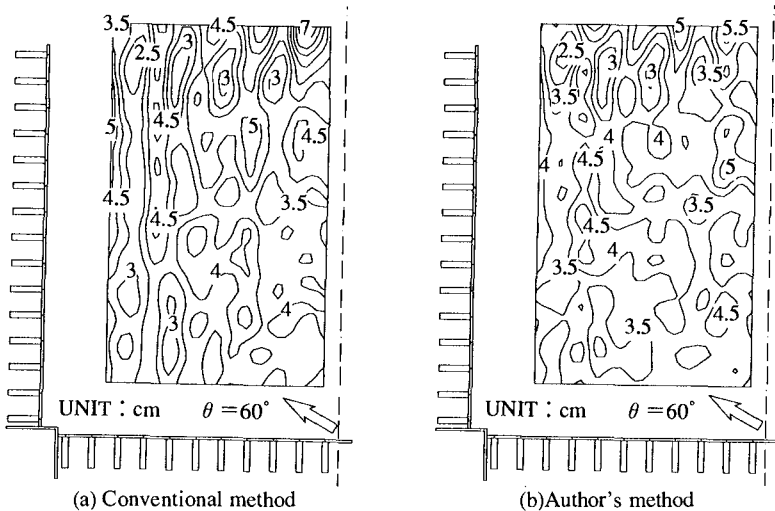


Fig.7 The contour of the wave heights
Regular wave: $T=1.5s, H=5cm, \theta=60^\circ$)

values. Thus, it is judged that both absorption controls had the same degree of absorptivity.

4.4 CAPABILITY OF NON-REFLECTED WAVE MAKER THEORY FOR MULTI DIRECTIONAL WAVES

The experiments were carried out to investigate capability of absorption for multi directional waves. WAVE MAKER1 and WAVE MAKER 2 generated multi directional waves and WAVE MAKER 3 absorbed waves propagating toward WAVE MAKER 3. WAVE MAKER 3 was driven by using author's method or conventional method for the sake of comparison. Furthermore WAVE MAKER 3 was controlled as the reflecting wall. The water elevations were measured by STAR ARRAY that was located in front of WAVE MAKER 3 (Fig.5). Directional spectrum were calculated by using Expanded Maximum Entropy Principle Method(EMEP). Since EMEP can not estimate the phase interaction of incident and reflected waves, STAR ARRAY was set over one wave length (2.7 m) distant away from WAVE MAKER 3.

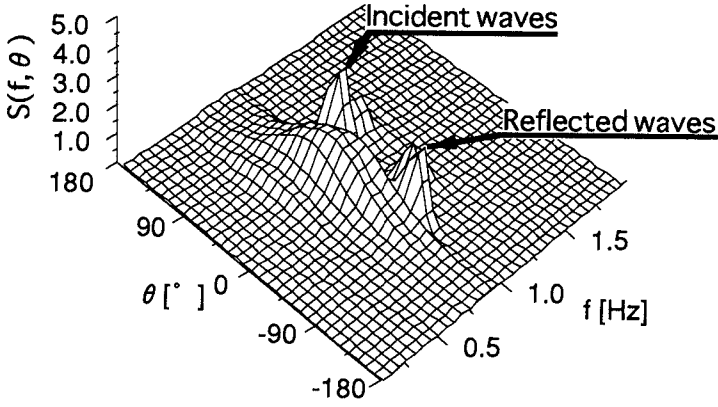
In the experiments, the wave generated by WAVE MAKER1 and 2 had Bretschneider-Mitsuyasu spectrum, Mitsuyasu type directional function ; $S_{max}=10,70$, $H_{1/3}=5\text{cm}$, $T_{1/3}=1\text{s}$ and $\theta_p=45^\circ$. S_{max} is spreading parameter, $H_{1/3}$ significant wave height, $T_{1/3}$ significant wave period, θ_p is principal wave direction.

Fig.10 shows the directional spectrum in the case of $S_{max}=70$. In the case of WAVE MAKER 3 being the reflecting wall (Fig.10 (a)), three peak frequency appear at around 0° , -45° and 45° . The wave direction of incident component waves appears at about 45° . Reflected component waves corresponding to the incident component waves propagate to the direction of -45° . The component wave of which frequency is about 0.9Hz can be understood as the component waves that propagate crosswise between WAVE MAKER 1 and 2. On the other hand, the reflected component waves less than 1.3Hz can not be seen in the case of author's method (Fig.10 (b)). This figure indicates that the author's method can absorb multi directional waves effectively. And the directional spectrum analysis showed the similar results for $S_{max}=10$ and $S_{max}=70$.

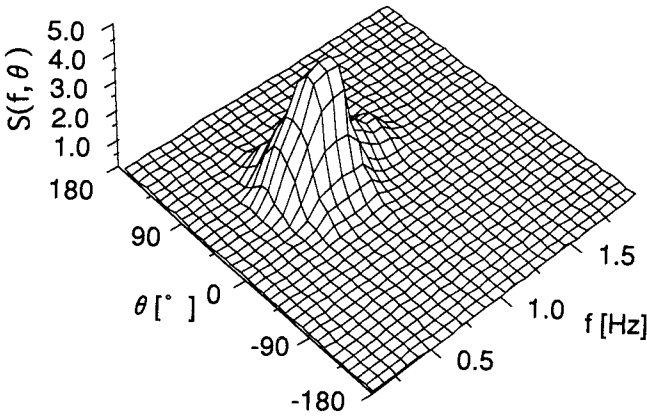
But, the results of directional spectrum analysis did not indicate the remarkable difference between author's method and conventional one.

The conventional method can effectively absorb the wave trains which propagate toward the wave paddles only at a right angle. But this can not absorb the wave trains coming obliquely to the wave paddles. Thus reflected waves should remain in the basin. Now we try to explain the reason why the directional spectrum could not show the remarkable difference between the author's method and the conventional one. In the calculation of directional spectrum, cross-spectrum must have presumption error and smoothing operation is indispensable for cross-spectrum analysis. Consequently, it is judged that the influence of the reflected waves vanished in the process of the calculation.

Fig.11 shows significant wave heights($h_1 \sim h_4$) at STAR ARRAY. Legends(●, ○, ■) indicate the difference of the control method of WAVE MAKER 3; ● for standstill as a wall, ○ for control by the author's method, ■ for control by the conventional one. As shown in figure($S_{max}=70$), each significant wave height does not show the large difference between the author's method and the conventional one and distribution of $H_{1/3}$ is uniform. But, for $S_{max}=10$, the significant wave heights of the conventional method is not specially uniform. This attributes to the disturbance caused by the reflected waves from WAVE MAKER 3. Therefore, we may conclude that as an angle between wave direction and wave paddle is large, the conventional method can not absorb oblique wave groups with such wave direction.



(a) Reflecting wall



(b) Author's method

Fig.10 The comparison of the directional spectrum($S_{max}=70$)

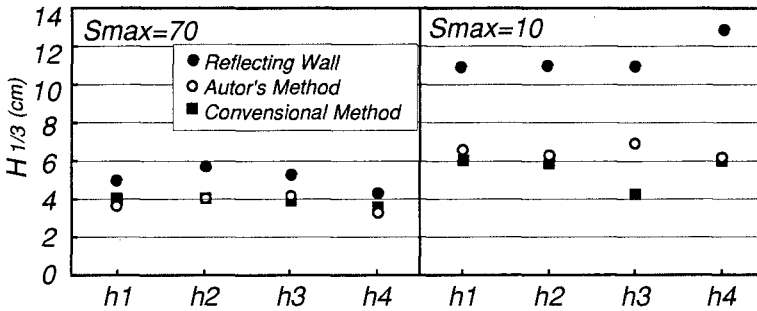


Fig.11 The comparison of the wave heights at STAR ARRAY

5. CONCLUSION

This paper established a non-reflected wave maker theory for multi-directional waves considering evanescent waves as well, using the data on water surface elevation at the front of two or more wave paddles and the past data. From the results of numerical calculation and experiments, this theory was proved to have higher absorptivity than the conventional method.

Acknowledgments

The authors also wish to thank Professor Masaru Mizuguchi at Chuo University for his helpful suggestions. The authors would like to express his gratitude to Mr. Takamitsu Noguchi, Mr. Masaki Anzai, and Mr. Hiroyuki Kishi of Taisei Service, Inc. for their cooperation.

References

- [1] T. Hiraishi (1991): Experimental Study on the Effective Test Area for Directional Waves by a Serpent-Type Wave Generator., Proc. of the Coastal Engineering, Vol.38, pp.126-130.(In Japanese).
- [2] T. Hiraishi (1990): Report on Wave Makers in Canada - Reclamation and Dredge, No.156, pp.30-38. (In Japanese).
- [3] T. Kawaguchi (1986): Absorbing Wave Making System with Wave Sensor and Velocity Control, Mitsui Zousen Technical Review., No.128, pp.20-24. (In Japanese).
- [4] H. Hiraguchi, R. Kajima, H. Tanaka, T. Ishii (1990): Wave Absorption of a Directional Wave Maker, Proc. of the Coastal Engineering, Vol.38, pp.121-125.(In Japanese).
- [5] T. Ikeya, Y. Akiyama, K. Imai (1992): Wave Absorption Theory for Multi-directional Waves, Proc. of the Coastal Engineering, Vol.39, pp.81-85.(In Japanese).
- [6] K. Ito, M. Isobe, H. Katsui (1994): Directional wavemaker theory that can absorb reflected waves, Proc. of the Coastal Engineering, Vol.41, pp.101-105.(In Japanese).
- [7] K. Ito, H. Katsui, M. Mochizuki, M. Isobe (1995): Experiment of Non-reflected Multi directional Wave Maker Disposed in to C-shape, Proc. of the Coastal Engineering (now being printed), Vol.42. (In Japanese).
- [8] H. Toida, Masaru M., Y. Moriya (1994): End Control Method for Making a Uniform Wave Field Using Multi-directional Wave Makers, Proc. of the Coastal Engineering, Vol.41, pp.106-109. (In Japanese).